Norman A. Fleck[1] *and James C. Newman, Jr.*[2]

Analysis of Crack Closure Under Plane Strain Conditions

REFERENCE: Fleck, N. A. and Newman, J. C., Jr., **"Analysis of Crack Closure Under Plane Strain Conditions,"** *Mechanics of Fatigue Crack Closure, ASTM STP 982,* J. C. Newman, Jr. and W. Elber, Eds., American Society for Testing and Materials, Philadelphia, 1988, pp. 319–341.

ABSTRACT: An elastic-perfectly plastic finite-element analysis has been conducted of plasticity-induced crack closure under plane strain conditions. At a load ratio R ($= K_{min}/K_{max}$) of zero, crack closure was observed in a center-cracked panel but not in a bend specimen. Crack closure in the center-cracked panel occurred for a transient period of growth as the crack evolved from the state of a stationary crack to the steady state of a growing fatigue crack. The influence of specimen geometry upon closure response was rationalized in terms of the "T-stress." This stress is the nonsingular constant second term in the near tip series expansion of the normal stress parallel to the crack plane. No closure was observed in the center-cracked panel for $R \geq 0.3$. The crack opening response and plastic zone distribution of a growing fatigue crack were compared with those of a cyclically loaded stationary crack and a statically loaded tearing crack. Some of the features of the solution for the growing fatigue crack were similar to the solution for a stationary crack, while other features bore more resemblance to those of a tearing crack.

KEY WORDS: crack closure, crack propagation, elastic-plastic fracture, fatigue, finite-element analysis, fracture, plane strain

The phenomenon of plasticity-induced crack closure is associated with the development of residual material on the flanks of an advancing fatigue crack. While it is easy to envisage that this residual material can come from the side faces of a specimen under plane stress conditions, it is difficult to discover the origin of this extra volume of material on the crack flanks when it is assumed that plane deformations occur and plastic flow is incompressible. The purpose of the present paper is to determine whether plasticity-induced fatigue crack closure occurs in an elastic-perfectly plastic body under plane strain conditions.

To fix our ideas, consider the small scale yielding (ssy) problem of a semi-infinite crack in an infinite body with the asymptotic boundary conditions that, outside the plastic wake

$$\sigma_{ij} \rightarrow Kr^{-1/2} f_{ij}(\theta) \quad \text{as } r \rightarrow \infty \tag{1}$$

where $\underline{\sigma}$ is the stress tensor, K is the stress intensity factor, and r and θ are polar coordinates centered at the crack tip, and the dimensionless functions f_{ij} are given by the elastic solution (Fig. 1). Assume that the crack suffers fatigue loading and has advanced from $x = -\infty$ to $x = 0$, where x and y are cartesian coordinates centered at the crack tip. It is now shown that a residual wedge of material of thickness $2h$ could lie along the crack flanks from $x =$

[1] Lecturer, Department of Engineering, University of Cambridge, Trumpington St., Cambridge CB2 1PZ, England.
[2] Senior research scientist, NASA Langley Research Center, Hampton, VA 23665.

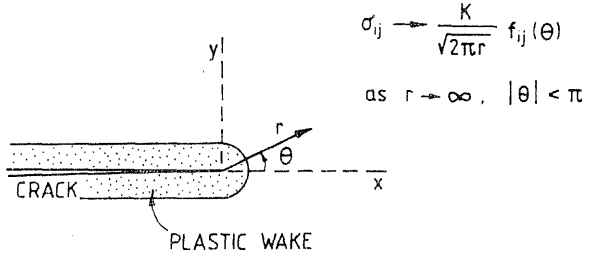

FIG. 1—*Fatigue crack growth in small-scale yielding.*

$-b$ where b is small to $x = -\infty$ and cause premature closure of the crack. The associated stress field caused by this wedge of material at zero applied load tends to zero like $1/r$, as $r \rightarrow \infty$, Tada et al. [*1*]. Equation 1 is not violated by this stress field, and so the solution is admissible within the context of small-scale yielding. The extra volume of material can come from infinity.

If a residual-plastic wedge of uniform thickness exists along the crack flanks, within the plastic wake the stress component σ_{xx} remains finite as $r \rightarrow \infty$. The argument is as follows. In the elastic region adjacent to the plastic wake, the strains decay as $1/\sqrt{r}$ as $r \rightarrow \infty$ (Fig. 1). Hence the sum of the elastic and the residual plastic strains in the plastic wake decays as $1/\sqrt{r}$. The strains within the plastic wake may have a finite plastic component, provided there exists an elastic component of equal magnitude and opposite sign. Associated with this finite elastic strain is a finite stress σ_{xx}. Hence, within the plastic wake, σ_{xx} remains finite and the magnitude of the residual plastic strains is less than that of the yield strain.

There is further evidence that plasticity-induced crack closure can occur under plane strain conditions. It is known that the crack opening displacement local to the crack tip in a steadily growing crack under constant K is less than the elastic crack opening, see for example Dean and Hutchinson [*2*]. Imagine that the crack opening profile for a fatigue crack at the maximum stress intensity of the fatigue cycle K_{max} is given by the solution for a steadily growing crack under constant $K = K_{max}$. Also assume that the crack unloads like an elastic crack. If this is the case then the crack closes prematurely at a tensile load, and plasticity-induced closure results.

Dimensional Analysis

The small-scale yielding approximation assumes that the crack tip field is a function only of K and is not dependent upon other details of the remote loading or geometry. Consider an elastic-perfectly plastic body of yield stress σ_y, Young's modulus E, and Poisson's ratio ν. Under ssy, the plastic zone size directly ahead of the crack tip r_p is given by

$$r_p = f(K, \sigma_y, E, \nu) \tag{2}$$

where f is an unknown function.

By dimensional analysis this reduces to

$$\frac{r_p}{K^2/\sigma_y^2} = f\left(\frac{\sigma_y}{E}, \nu\right) \tag{3}$$

where the dependence of $r_p/(K^2/\sigma_y^2)$ on σ_y/E and ν is considered to be small.

Larsson and Carlsson [3] have examined the general validity of Eq 3 by determining the plastic zone size in a number of specimen configurations, using the finite element method. In each case, the loading was less than the ASTM limit (ASTM Test Method for Plane-Strain Fracture Toughness of Metallic Materials [E 399]), $K < \sigma_y \sqrt{a/2.5}$. Thus the plastic zone size was always much smaller than the crack length. They found large differences in plastic zone size from one specimen to the next for the same value of K. Larsson and Carlsson accounted for this variation as follows. The stress state at a crack tip in an elastic body is given by Eq 1 and higher order nonsingular terms

$$\sigma_{xx} = \frac{K}{\sqrt{2\pi r}} f_{xx}(\ ) + T + 0(r) \tag{4}$$

while for other stress components

$$\sigma_{ij} = \frac{K}{\sqrt{2\pi r}} f_{ij}(\theta) + 0(r)$$

The term T is independent of r, is linear in the remote applied stress, and is a function of specimen configuration including crack length. Larsson and Carlsson determined the "T-stress" for several specimen geometries and showed that this stress was the cause of the variation in plastic zone size between specimens. Thus, Eq 3 is replaced by

$$\frac{r_p}{K^2/\sigma_y^2} = f\left(\frac{T}{\sigma_y}, \frac{\sigma_y}{E}, \nu\right) \tag{5}$$

Similarly, the crack opening displacement δ a distance x from the crack tip is given by

$$\frac{\delta}{K^2/\sigma_y E} = f\left(\frac{x}{K^2/\sigma_y^2}, \frac{T}{\sigma_y}, \frac{\sigma_y}{E}, \nu\right) \tag{6}$$

Larsson and Carlsson [3] and Rice [4] found that δ is only slightly dependent upon specimen geometry: $\delta/(K^2/\sigma_y E)$ varies weakly with T/σ_y in a quadratic manner.

In the present study, several types of loading were applied to a center-cracked panel (CCP) and to a cracked bend specimen:

(1) stationary crack, loaded monotonically and cyclically,
(2) tearing crack, under constant K, and
(3) growing fatigue crack under constant ΔK.

In each case the solution was a function of specimen geometry. It is now postulated that the reason for the specimen dependence is that T/σ_y varies from one geometry to the next. For the case of a tearing crack, which has grown a distance Δa under constant K, Eqs 5 and 6 become

$$\frac{r_p}{K^2/\sigma_y^2} = f\left(\frac{\Delta a}{K^2/\sigma_y^2}, \frac{T}{\sigma_y}, \frac{\sigma_y}{E}, \nu\right) \tag{7}$$

and

$$\frac{\delta}{K^2/\sigma_y E} = f\left(\frac{x}{K^2/\sigma_y^2}, \frac{\Delta a}{K^2/\sigma_y^2}, \frac{T}{\sigma_y}, \frac{\sigma_y}{E}, \nu\right) \tag{8}$$

For a fatigue crack that has grown a distance Δa under a constant stress intensity range $\Delta K = K_{max} - K_{min}$, Eqs 5 and 6 become

$$\frac{r_p}{K_{max}^2/\sigma_y^2} = f\left(R, \frac{\Delta a}{K_{max}^2/\sigma_y^2}, \frac{T_{max}}{\sigma_y}, \frac{\sigma_y}{E}, \nu\right) \tag{9}$$

and

$$\frac{\delta}{K_{max}^2/\sigma_y E} = f\left(\frac{x}{K_{max}^2/\sigma_y^2}, R, \frac{\Delta a}{K_{max}^2/\sigma_y^2}, \frac{T_{max}}{\sigma_y}, \frac{\sigma_y}{E}, \nu\right) \tag{10}$$

where $R = K_{min}/K_{max}$, and T_{max} is the T-stress at maximum load of the fatigue cycle. Finally, the ratio of crack opening load P_{op} to maximum load P_{max} for the growing fatigue crack may be expressed as

$$\frac{P_{op}}{P_{max}} = f\left(R, \frac{\Delta a}{K_{max}^2/\sigma_y^2}, \frac{T_{max}}{\sigma_y}, \frac{\sigma_y}{E}, \nu\right) \tag{11}$$

In the present study results are presented in the nondimensional form given by the above equations. The aim of the study is to answer the following questions:

1. Does a growing fatigue crack resemble more a stationary crack or a tearing crack?
2. Does plasticity-induced crack closure occur under plane strain conditions?

To answer these questions a finite-element analysis was conducted of stationary cracks, tearing cracks, and growing fatigue cracks.

Finite Element Analysis

An elastic-perfectly plastic, plane strain finite-element analysis was performed for the CCP and bend specimens (Fig. 2*a*). The finite-element model of these specimens was composed of 1967 two-dimensional, constant strain, triangular elements with 2114 degrees of freedom. Near the crack tip, the triangular elements were arranged to form a series of squares and their diagonals (Fig. 2*b*). Nagtegaal et al. [*5*] found that such an arrangement meets the incompressibility requirements associated with large plastic strains. Other arrangements of the elements can lead to plane strain locking of the elements, with stresses oscillating wildly from one element to the next.

Fictitious springs were used to change the boundary conditions associated with crack growth, crack closure or crack opening. For free nodes along the crack surfaces, the spring stiffness was set to zero, and for fixed nodes, the stiffness was assigned extremely large values, see Newman [*6*] for details. When plotting plastic zone distributions, it was assumed that an element had yielded when the effective stress in the element was greater than 0.98 σ_y. A more stringent criterion led to the frequent occurrence of an elastic element surrounded by plastic elements, which is physically unacceptable. Yield was defined by the von Mises criterion.

In most cases, the cracks were grown at constant K or at constant cyclic K from an initial crack length a of 0.491 w to a final crack length of 0.506 w, where w is the specimen width (Fig. 2*a*). The yield stress of the material σ_y was fixed at $E/200$, and Poisson's ratio ν was 0.3; these are typical values for a high strength aluminum alloy. The applied stress intensity factor K for static loading and K_{max} for fatigue loading were 0.44 $\sigma_y \sqrt{w}$, which is just

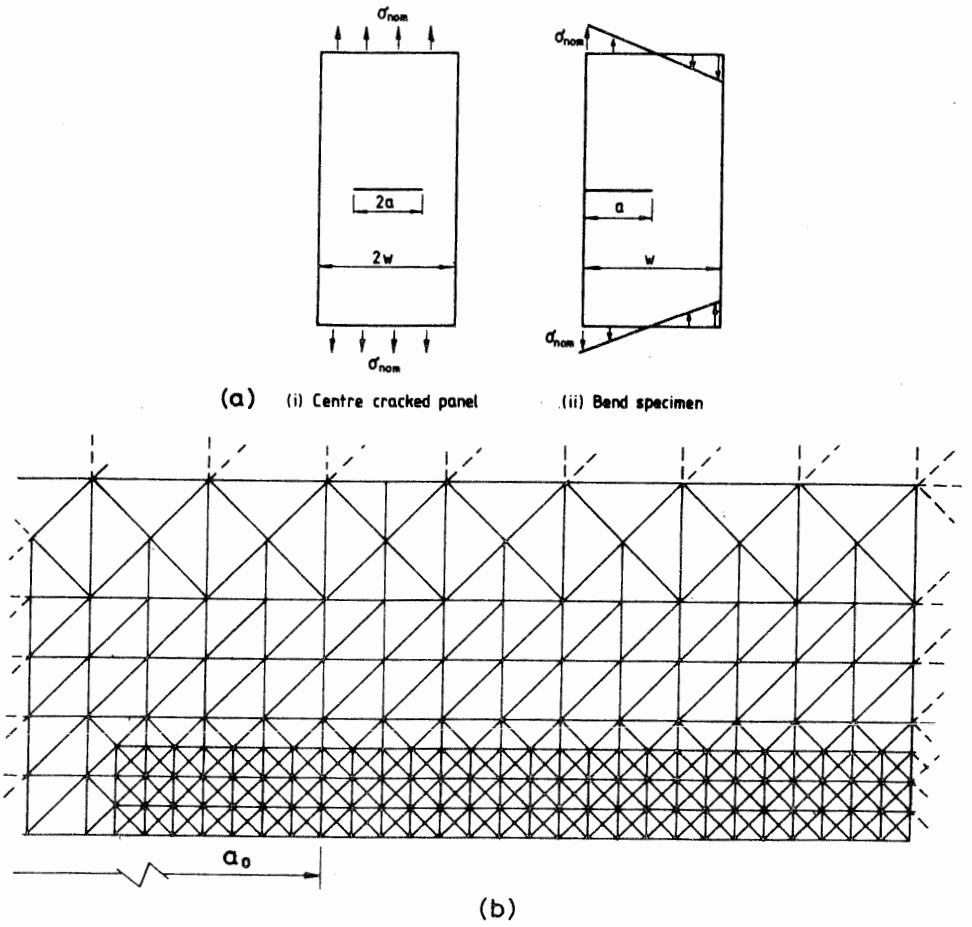

FIG. 2—(a) *Specimen configurations analyzed and* (b) *mesh near crack tip.*

below the ASTM limit of 0.45 $\sigma_y \sqrt{w}$ for fracture test correlation in terms of K values (ASTM E 399).

It was assumed that the crack tip element size of 0.00078125 w was sufficiently small for the analysis to give accurate results. Typically, the plastic zone directly ahead of the crack extended over more than 10 element sizes, and the total number of yielded elements exceeded 200. Newman [*6*] has found that this size of mesh yields accurate results under the same applied K and plane stress conditions.

A preliminary elastic analysis showed that the stress concentration factor for both geometries was 34, for $a/w = 0.5$. The finite-element analysis predicted crack opening displacements about 5% less than the exact solution for both geometries, reflecting the upper bound nature of the numerical calculation. The ratio $T\sqrt{w}/K$ was also determined from the elastic analysis, using the procedure of Larsson and Carlsson [*3*] as follows. Considering Eq 4, we have $f_{xx}(\pi) = 0$, thus a plot of the nodal average stress σ_{xx} versus distance r behind the crack tip yields the quantity $T + 0(r)$. For $r/a < 0.2$, σ_{xx} is almost constant, and the value of σ_{xx} extrapolated to $r = 0$ gives T. For $a/w = 0.5$ it was found that $T\sqrt{w}/K = -0.786$ ($T/\sigma_{nom} = -1.14$) for the center-cracked panel, while $T\sqrt{w}/K = 0.160$ ($T/\sigma_{nom} = 0.294$) for the bend specimen. The nominal applied stress σ_{nom} is defined in Fig. 2*a*. The value of T/σ_{nom} for the center-cracked panel is 6% less than the value quoted by Larsson and Carlsson [*3*] for the same geometry; the agreement is acceptable.

Results for the elastic-perfectly plastic analysis are now given, first for a stationary crack, then for a tearing crack, and finally for a growing fatigue crack.

Stationary Crack

The crack opening response and plastic zone size was determined for a cyclically loaded stationary crack of length 0.4906 w. Both the bend and CCP specimens were loaded to $K_{max} = 0.44\ \sigma_y \sqrt{w}$ and then unloaded to 0.8 K_{max}, 0.5 K_{max}, and to zero load.

Consider first the crack opening displacement at K_{max} (Fig. 3*a*). Recent finite-element results by Sham [*7*] for the ssy problem are included in the figure. It appears that there is a small influence of specimen geometry upon crack opening, which may be accounted for in terms of a variation of T/σ_y between specimens. The crack opening, $\delta/(K_{max}^2/\sigma_y^2)$, is 10% greater for the CCP specimen ($T/\sigma_y = -0.35$) than for the bend specimen ($T/\sigma_y = 0.070$), with the small-scale yielding solution of Sham ($T/\sigma_y \approx 0$), lying between the two. The correlation with Sham's results suggests that the mesh is sufficiently fine for the load levels considered.

The plastic zone size at K_{max} is much larger for the CCP geometry (Fig. 4*a*), than for the bend specimen (Fig. 4*b*), in agreement with the findings of Larsson and Carlsson [*3*]. This is consistent with the elastic solutions for the center-cracked panel, where the effective stresses in the region of the crack tip are increased by the negative T-stress. In similar fashion, the effective stresses near the crack tip in an elastic bend specimen are lowered by the positive T-stress.

Now consider unloading from K_{max}. For both geometries, the reversed plastic zone grows in size with unloading, until it is about ¼ of the forward plastic zone at $K_{min} = 0$ (Fig. 4*a* and *b*). The reversed plastic zone size is in reasonable agreement with the prediction of Rice [*8*], where the reversed plastic zone size is calculated from the formula for the forward plastic zone size, with K_{max} replaced by ΔK and σ_y replaced by $2\sigma_y$. Rice has also suggested that the cyclic crack opening displacement $\Delta\delta = \delta_{max} - \delta_{min}$ should correlate with δ_{max} when $\Delta\delta$ is plotted as $\Delta\delta/(\Delta K^2/2E\sigma_y)$ versus $x/(\Delta K^2/4\sigma_y^2)$, and δ_{max} is plotted as $\delta_{max}/(K_{max}^2/E\sigma_y)$ versus $x/(K_{max}^2/\sigma_y^2)$. It is clear from Fig. 3*b* that the correlation is fair; the cyclic crack opening, $\Delta\delta/(\Delta K^2/2E\sigma_y)$, lies about 10% below the maximum crack opening displacement,

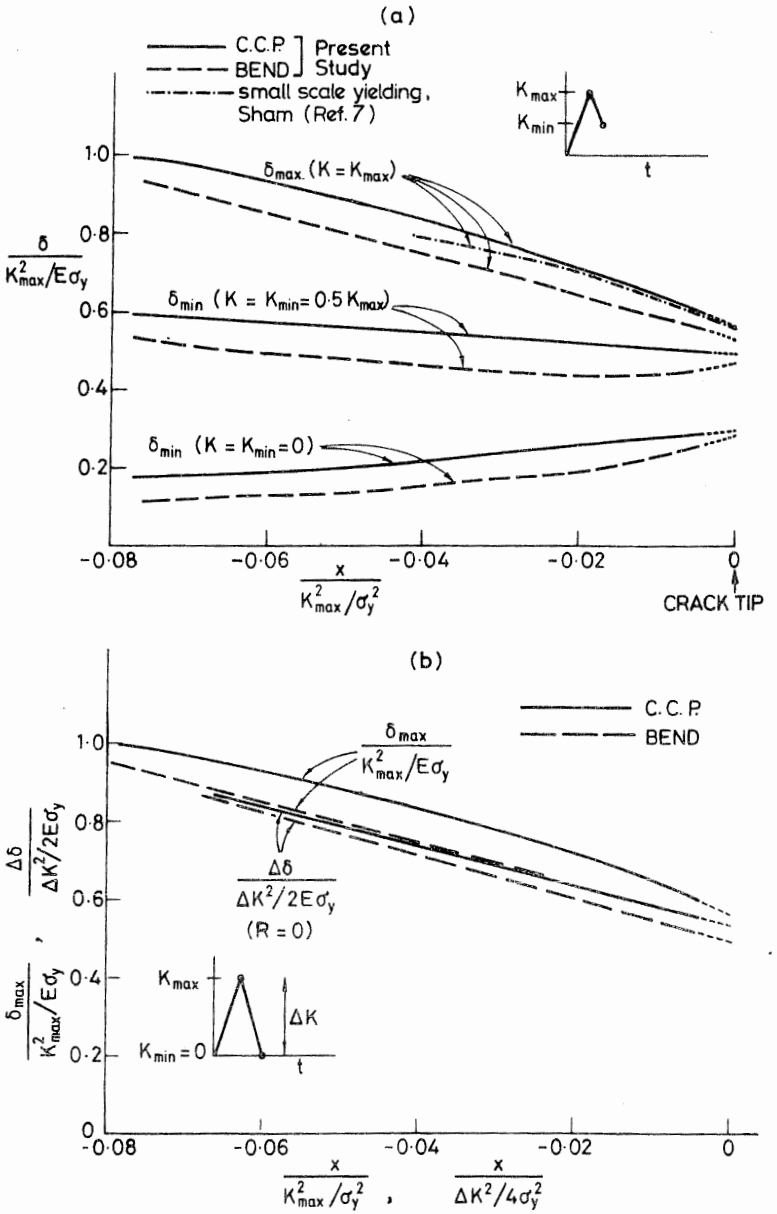

FIG. 3—(a) *Crack opening profile for a stationary crack, loaded to* K_{max} *and then unloaded to* K_{min}. (b) *Comparison of monotonic and cyclic crack opening response of a stationary crack.*

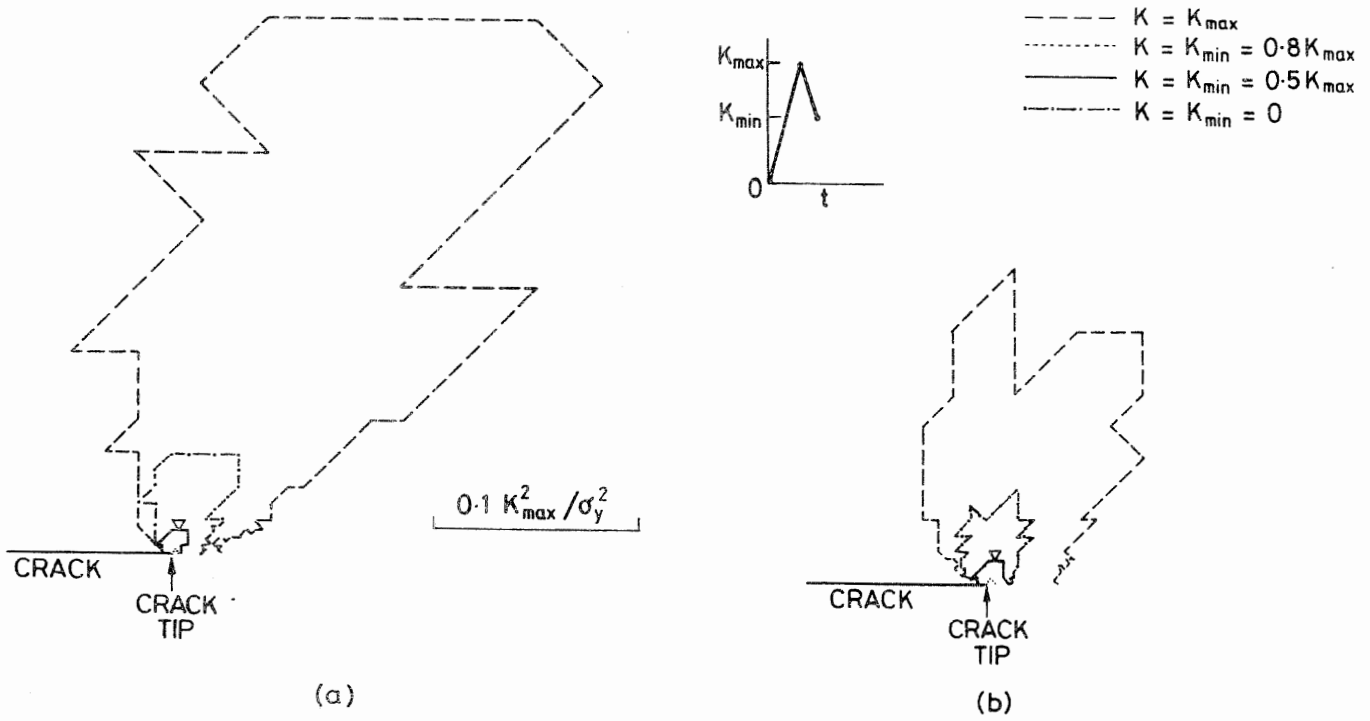

FIG. 4—*Plastic zone distribution at tip of stationary crack, loaded to* K_{max} *and then unloaded to* K_{min}: (a) *CCP and* (b) *bend specimen.*

$\delta_{max}/(K_{max}^2/E\sigma_y)$. The crack in the center-cracked panel is slightly more open at all load levels, than in the bend specimen (Fig. 3*a*). At zero load, the cracks remain fully open in both geometries: crack advance must occur before there can be the possibility of crack closure under tensile-tensile cyclic loading.

Tearing Crack

For a stationary crack in an elastic-plastic solid the strains increase as $1/r$ as the distance from the crack tip is diminished, and the crack has a finite opening at its tip [*9*]. For a growing crack, the strain singularity is weaker, $\ln(1/r)$, and the crack opening is of the form [*7,10*]

$$\delta = 5.462 \frac{\sigma_y}{E} r \ln \frac{\rho}{r} \tag{12}$$

where ρ is indeterminate from the asymptotic analysis.

The influence of specimen geometry upon the growth of a crack under constant remote K was investigated as follows. Crack growth by an amount $\Delta a = 0.080\ K_{max}^2/\sigma_y^2$ was simulated by releasing 20 successive crack tip nodes from an initial crack length a_o of 0.4906 w. The remote load was shed between the release of each node in order to preserve a constant remote K of 0.44 $\sigma_y \sqrt{w}$. The crack opening displacement responses are given in Fig. 5 and the plastic zone sizes in Fig. 6*a* and *b*. Included in Fig. 5 is the steady crack growth ssy solution ($T/\sigma_y = 0$) given by Dean and Hutchinson [*2*]. Dean and Hutchinson have confirmed that the crack opening displacement approaches zero as $r \ln \rho/r$ as $r \to 0$, in accordance with the exact asymptotic analysis (Eq 12). While the shape of the near tip

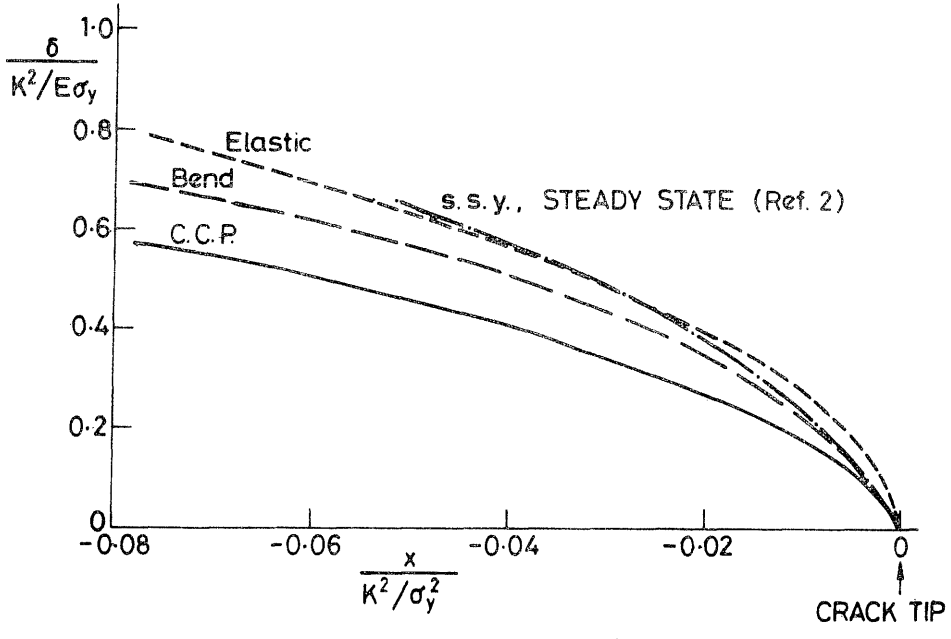

FIG. 5—*Crack opening response of a tearing crack, grown at constant* K.

crack opening for the bend and CCP geometries is similar to that given by Dean and Hutchinson, the size of the crack opening is less (Fig. 5). An examination of the crack opening with successive node release operations indicated that δ increased steadily with crack advance; thus it is likely that the curves for the bend and CCP geometries will be closer to the ssy steady state solution, as steady state conditions are attained. For the tearing crack, the crack opening displacement for the bend specimen is 20% greater than for the CCP geometry. This contrasts with the stationary crack response (Fig. 3*a*), where the crack opening is greater in the CCP specimen than in the bend specimen. For all geometries the crack opening near the crack tip is less for the growing crack than for a crack in a linear elastic body.

The evolution of plastic zone size with crack growth is shown in Fig. 6*a* for the CCP geometry, and in Fig. 6*b* for the bend geometry. Initially, $a = a_o$, and the crack tip plastic zone is that of a stationary crack. At $a = a_f$, the crack has grown by 20 element sizes ($\Delta a = a_f - a_o = 0.080\ K_{max}^2/\sigma_y^2$), and has taken on the character of a tearing crack.

Consider the case of the grown crack, at $a = a_f$. A secondary active plastic zone is present alongside the crack flanks. Within this zone the stress state is essentially $\sigma_{xx} = \sigma_y$, $\sigma_{yy} = 0 = \tau_{xy}$. This secondary plastic zone, separated by an elastic region from the primary zone in front of the crack tip, is a well-known feature of tearing cracks [*7,10*]. In order to understand why this secondary loading zone is required, we shall consider the stress-strain state of a fixed material point as the crack tip moves past it. Fix the reference frame with respect to the moving crack tip and consider the trajectory of the material point along Path 1 in Fig. 6*b*. As the material element moves from Point A to Point B it suffers a large tensile plastic strain in the *y*-direction, ϵ_{yy}^{pl}, and a large negative strain, ϵ_{xx}^{pl}. Equation 1 dictates that the sum of the elastic strain ϵ_{xx}^{el} and the plastic strain ϵ_{xx}^{pl} must tend to zero as $r \to \infty$ along $\theta = \pi$. Thus a secondary plastic zone is required to increase ϵ_{xx}^{pl} and decrease ϵ_{yy}^{pl} to an elastic order of magnitude, as the particle moves from *B* to *C* and thence to $r = \infty$ along $\theta \approx \pi$.

Now consider the deformation history of a material point along Path 2 in Fig. 6*b*, in order to discover why the secondary plastic zone can be much smaller than the primary plastic zone. As a material element moves from D to E along Path 2 it suffers a tensile plastic strain ϵ_{yy}^{pl} and a compressive strain ϵ_{xx}^{pl} both of magnitude less than the yield strain. Elastic strains are sufficient to reduce ϵ_{xx} and ϵ_{yy} to zero as the material point continues along Path 2 to $r = \infty$, $\theta = \pi$.

It is clear from Figs. 6*a* and *b* that the primary plastic zone ahead of the crack tip is larger for the CCP specimen than for the bend specimen, while the converse is true for the secondary plastic zone. These differences may be rationalized successfully in terms of the different T/σ_y values given by the elastic solutions. A large negative value of T/σ_y induces larger effective stresses near the crack tip, and an increased primary plastic zone size. A negative *T*-stress also suppresses formation of the secondary plastic zone wherin $\sigma_{xx} \approx \sigma_y$ and $\sigma_{yy} \approx 0 \approx \tau_{xy}$.

Simulation of Fatigue Crack Growth

Crack advance was simulated in the bend and CCP specimens using the loading scheme illustrated in Fig. 7. Each fatigue cycle consisted of

1. Apply maximum load to give the desired K_{max}.
2. Release a node under constant load, to simulate crack advance over one element dimension.
3. Unload to K_{min}. δ_{min} is the crack opening displacement defined at this point.

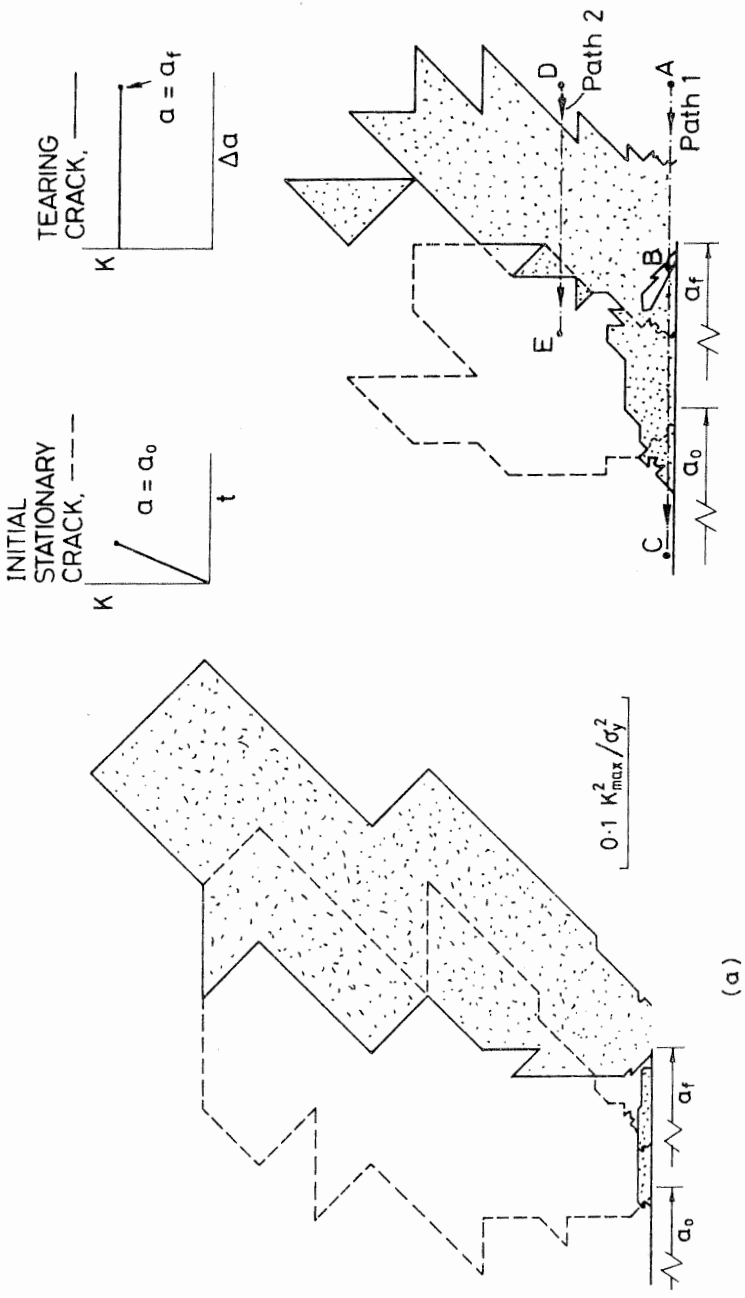

FIG. 6—*Evolution of plastic zone with crack growth:* (a) *CCP and* (b) *bend specimen.*

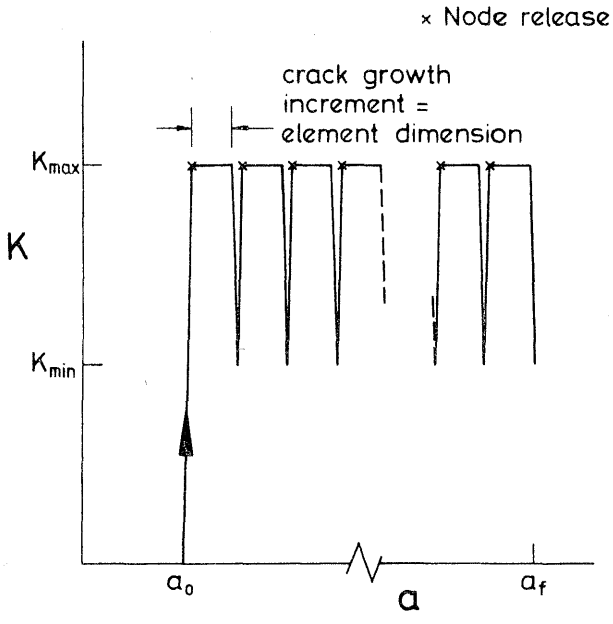

FIG. 7—*Simulation of fatigue crack growth.*

4. Reload to K_{max}. δ_{max} is the crack opening displacement defined at this point, and $\Delta\delta = \delta_{max} - \delta_{min}$.
5. Release the next node and continue as above.

Three load ratios were considered, $R = 0$, 0.5, and 0.8. In general, a crack was grown over 20 of the smallest elements (each of size 0.00078125 w), from an initial crack length a_o of 0.4906 w to a final crack length a_f of 0.5063 w. For each load ratio, the crack opening behavior and the plastic zone distribution were examined in order to determine whether a growing fatigue crack resembles more a stationary crack or a tearing crack.

Crack Opening Behavior

The crack opening response of the fatigue crack after 20 growth steps is summarized in Figs. 8 through 12. Consider first Figs. 8*a* through *c* where δ_{max} and δ_{min} are given as a function of R and geometry. At all R, the bend specimen shows larger crack openings than the CCP specimen, in agreement with the tearing crack response. For both the bend and the CCP geometries the crack remains fully open at K_{min}, for $R = 0.8$ (Fig. 8*a*). At $R = 0.5$ (Fig. 8*b*), the crack in the bend specimen is fully open at K_{min} while the crack in the CCP specimen is shut over one element dimension at K_{min}. At $R = 0$ (Fig. 8*c*), the crack in the bend specimen is shut over one element dimension, while the crack in the CCP specimen is shut from its tip to approximately the initial position a_o of the crack tip. The associated compressive stresses acting across the crack flanks at $K_{min} = 0$ in the CCP specimen are included in Fig. 8*c*.

It is likely that closure over a single element dimension is an artifact of the finite-element discretization, and the manner by which fatigue crack growth is simulated. By releasing a

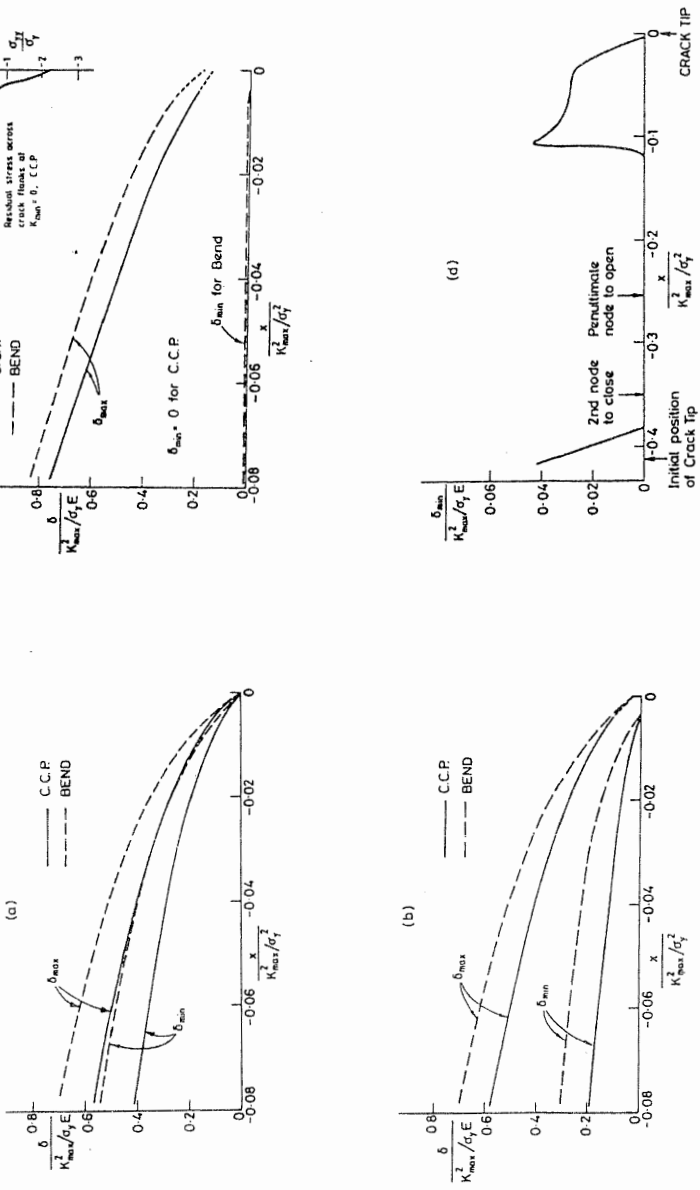

FIG. 8—*Crack opening response of a growing fatigue crack, after a crack growth increment* Δa *of 0.080* K_{max}^2/σ_y^2: (a) R = *0.8*, (b) R = *0.5*, (c) R = *0, and* (d) δ_{min} *for* R = *0, after* $\Delta a = 0.414\ K_{max}^2/\sigma_y^2$: *The node behind crack tip is first to close and last to open.*

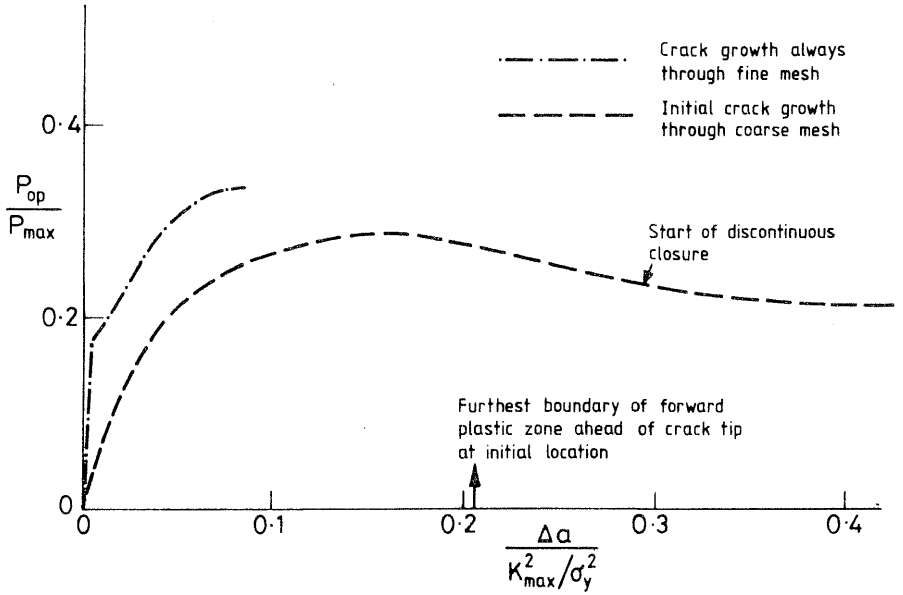

FIG. 9—*Closure transient of CCP geometry:* $K_{max} = 0.44\ \sigma_y \sqrt{w}$, R = 0.

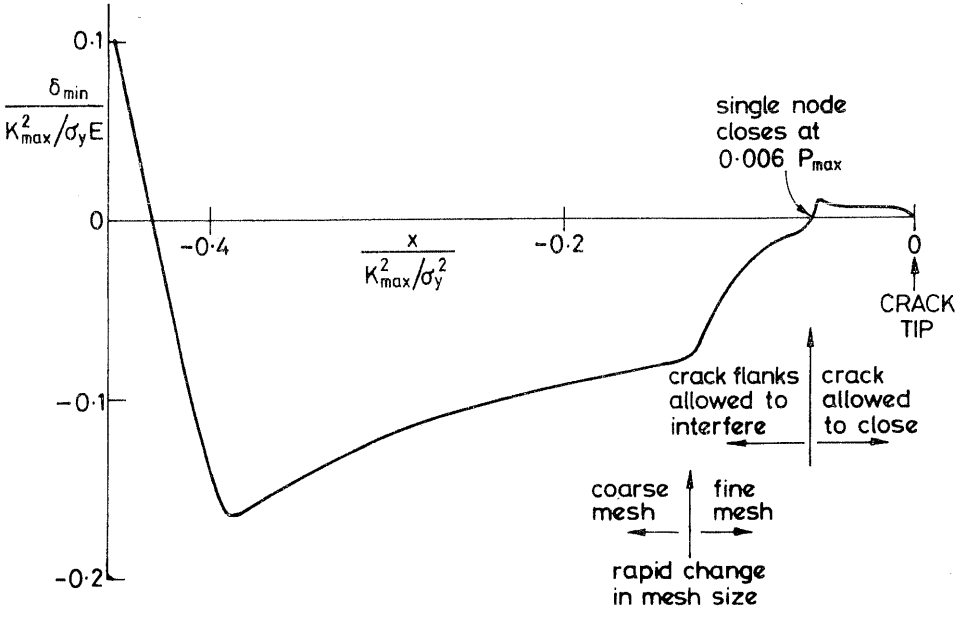

FIG. 10—*Crack profile in CCP geometry after a crack growth increment* Δa *of 0.414* K_{max}^2/σ_y^2. $K_{max} = 0.44\ \sigma_y \sqrt{w}$, *and* R = 0. *Crack allowed to close over only first 15 elements back from the crack tip.*

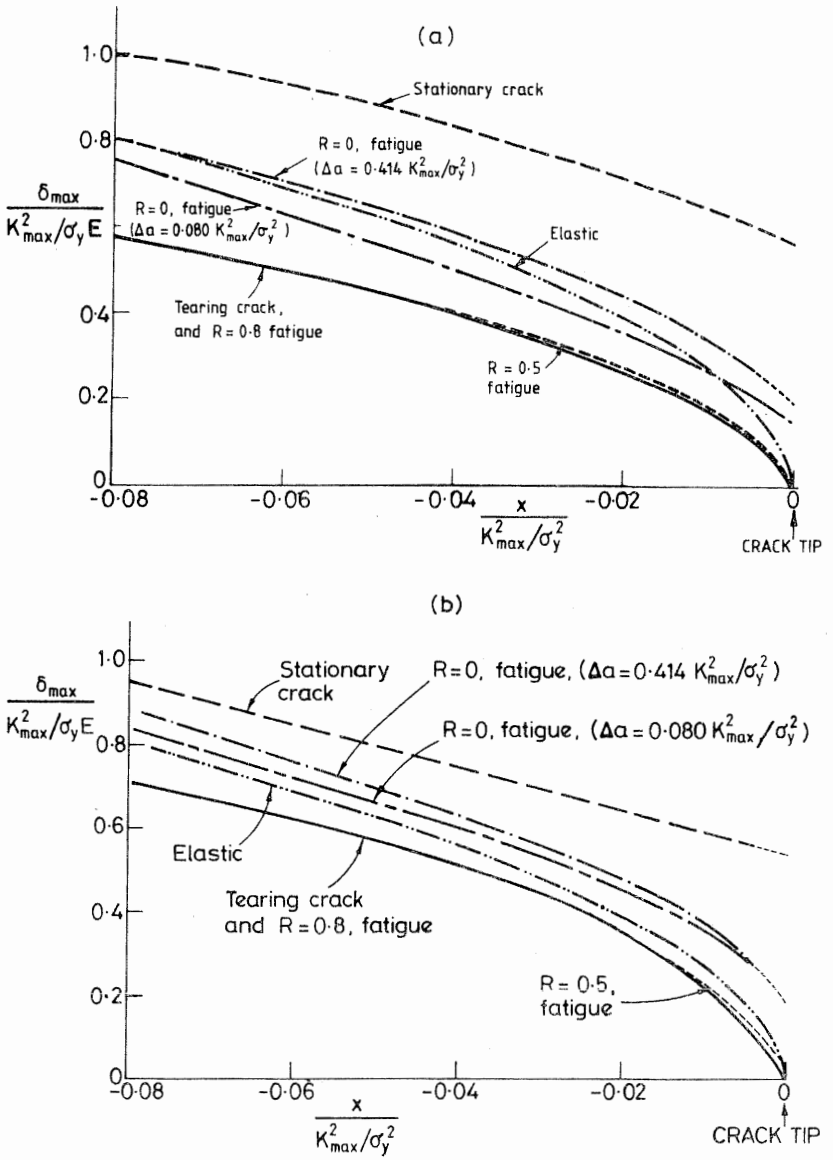

FIG. 11—*Comparison of crack opening response of a growing fatigue crack at* $K = K_{max}$ *with that of a tearing crack at constant* $K = K_{max}$. *Unless otherwise stated,* $\Delta a = 0.080\ K_{max}^2/\sigma_y^2$ *for the fatigue crack and for the tearing crack:* (a) *CCP and* (b) *bend geometry.*

node at maximum load, large residual tensile strains ϵ_{yy}^{pl} are left in the unloaded crack tip element. This results in an abnormally high closure load for this element. Thus it is assumed that the crack is still open when closure occurs over a single crack tip element dimension at K_{min}. This assumption was verified by the following numerical experiment. A crack was grown in the bend specimen over 20 small element sizes using a K_{max} of $0.44\ \sigma_y \sqrt{w}$ and a K_{min} of zero. Then the crack was held stationary and cycled ten times with the same K_{max}

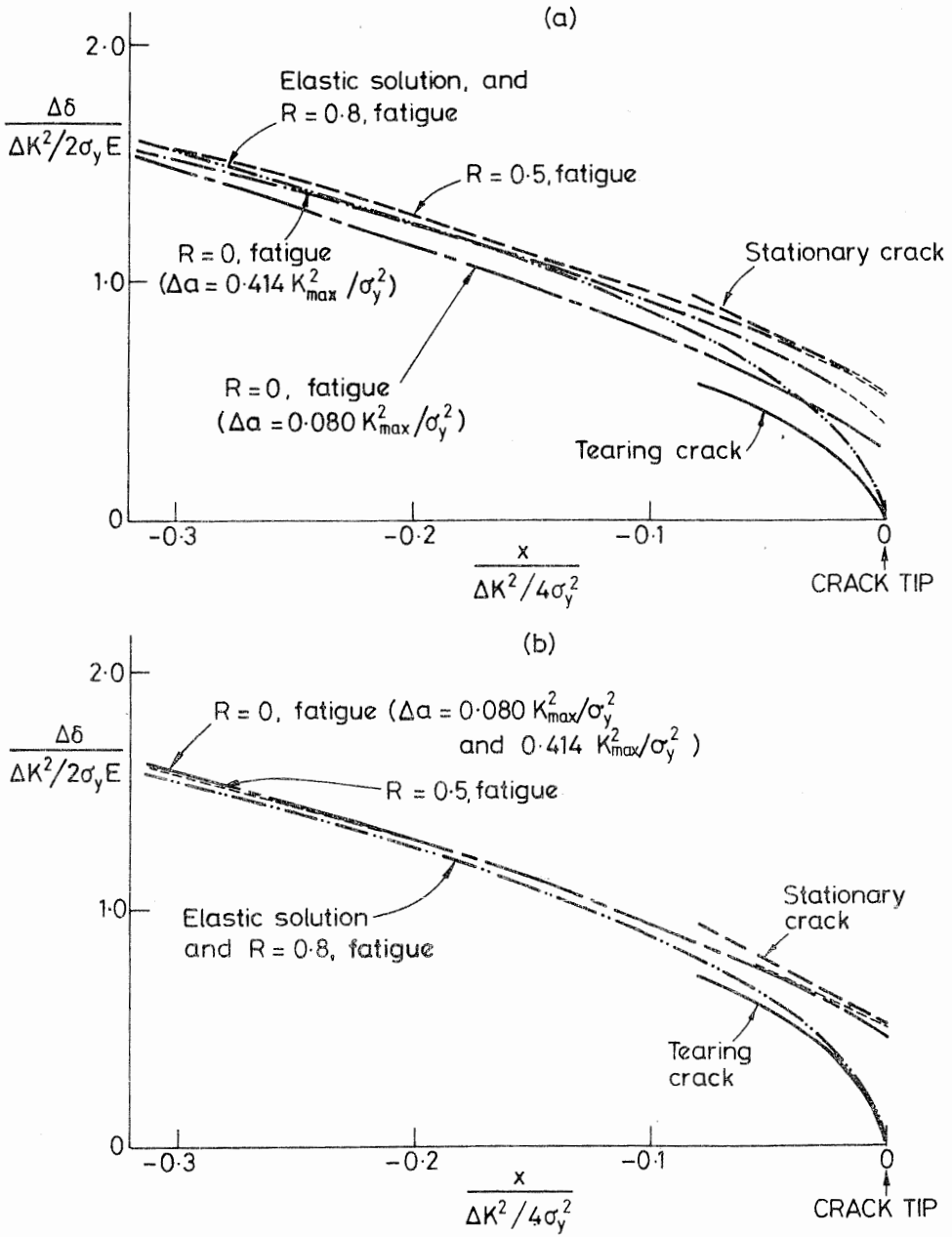

FIG. 12—*Comparison of cyclic crack opening response of growing fatigue crack with the cyclic response of a stationary crack, and the inferred cyclic response of a tearing crack. Unless otherwise stated,* $\Delta a = 0.080\ K_{max}^2/\sigma_y^2$ *for the fatigue crack and for the tearing crack:* (a) *CCP and* (b) *bend geometry.*

and K_{min} as before. The crack opening load for the single element behind the crack tip decreased from 0.19 P_{max} to less than 0.02 P_{max} during the ten cycles with the crack held stationary. It is concluded that only the CCP specimen displays plasticity-induced crack closure at $R = 0$.

Ogura et al. [*11*] have also simulated fatigue crack growth under plane strain conditions, using the finite-element method. They found that P_{op}/P_{max} stabilized to a constant value after some crack growth. Their results are questioned as the ratio of plastic zone size to element size was much smaller in their study than in the present study.

The crack opening load P_{op} normalized by P_{max} is given in Fig. 9 for the CCP specimen, at $R = 0$. The crack closure load P_{cl} is not displayed, as P_{cl} is sensitive to the load at which the crack tip node is released and to the mesh size [*6*]. It appears from Fig. 9 that P_{op}/P_{max} rises to a value of 0.32 as the fatigue crack is advanced by $\Delta a = 0.080\ K_{max}^2/\sigma_y^2$ over 20 small element sizes. In order to determine whether P_{op}/P_{max} stabilized at this value, the fatigue crack was grown over a much larger distance of $\Delta a = 0.414\ K_{max}^2/\sigma_y^2$, as follows. The crack was advanced through the coarse part of the mesh and into the fine part of the mesh, from an initial length of 0.425 w. After a release of 51 successive nodes the crack attained the same final position as before. Results are given in Fig. 9. It is deduced that P_{op}/P_{max} increases with Δa more slowly through the coarse mesh than through the fine mesh. A peak in P_{op}/P_{max} is displayed when the crack has advanced by approximately the maximum extent of the plastic zone associated with the stationary crack at a_o. With further crack advance, P_{op}/P_{max} decays again.

The crack opening response of the CCP specimen at $\Delta a = 0.414\ K_{max}^2/\sigma_y^2$ was examined in order to elucidate the closure process. The node behind the crack tip closed at 0.16 P_{max}, followed by a node near a_o at 0.09 P_{max}. At zero load the crack showed "discontinuous closure," whereby the crack was open near its tip and closed further back near a_o (Fig. 8*d*). On increasing the load again, the nodes near a_o opened when the load was 0.13 P_{max}, followed by the node behind the crack tip at 0.22 P_{max}. It appears that a residual wedge of stretched material has been left on the crack flanks at the location of the forward plastic zone associated with the initial crack length.

This wedge of material appears to be the cause of the closure phenomenon. It is formed during the initial period as the crack evolves from the state of a stationary crack to the steady state of a growing fatigue crack. When the crack has advanced a small distance ahead of its initial position ($\Delta a/(K_{max}^2/\sigma_y^2) < 0.3$, Fig. 9), the crack closes continuously. After further advance the crack closes discontinuously.

In order to determine whether the crack opening load tends to zero in Fig. 9 at large Δa, the finite-element program was modified as follows. The crack was allowed to close and induce compressive stresses across the crack flanks over only 15 small element sizes back from the crack tip. At greater distances from the crack tip, the crack flanks were allowed to overlap and not induce any closure stresses. If plasticity-induced crack closure is a transient phenomenon, associated with a residual wedge of material near a_o, then this procedure will lead to the closure load quickly becoming zero after a small amount of crack advance. The resulting crack profile for the CCP specimen at $K_{min} = 0$ is shown in Fig. 10, after a crack growth increment of Δa of $0.414\ K_{max}^2/\sigma_y^2$. The crack is open near its tip, with a single node experiencing closure stresses 15 elements back from the crack tip. This node closed at zero load to within the accuracy of the analysis. Further back from the crack tip, the crack flanks overlap indicating the approximate form of the residual wedge of material on the crack flanks near a_o. The perturbation in the shape of this residual wedge at $x = -0.13\ K_{max}^2/\sigma_y^2$ is due to a rapid change in mesh refinement at this location. It is concluded from Fig. 10 that it is only the residual wedge of material near a_o, which induces crack closure. At large Δa, it seems that the closure load decays to zero. This behavior contrasts with the corre-

sponding results for plane stress conditions [6]. There, P_{op}/P_{max} increased monotonically to a stabilized positive value after a transient period of crack growth, for $-1 \leqq R \leqq 0.5$.

Comparison of Growing Fatigue Crack with Stationary and Tearing Cracks—The crack opening behavior of the growing fatigue crack is compared with that of the stationary crack and the tearing crack in Figs. 11 and 12. The data are taken from previous graphs; unless otherwise stated, a crack growth increment of $0.080\ K_{max}^2/\sigma_y^2$ is assumed.

It is clear from Fig. 11*a* for the CCP geometry and from Fig. 11*b* for the bend specimen that δ_{max} for a growing fatigue crack resembles that of a tearing crack more than that of a stationary crack, at all R. Only at $R = 0$ does the fatigue crack show a significant opening at its tip; in this case, the extrapolated crack tip opening displacement is less than half the value for a stationary crack at the same K_{max}.

The cyclic crack opening response of the growing fatigue crack is compared with the cyclic response of the stationary crack and tearing crack in Fig. 12*a* for the CCP geometry and in Fig. 12*b* for the bend specimen. The cyclic response of the stationary crack is taken from Fig. 3*b*, while the "cyclic response of the tearing crack" is deduced from the curves of Fig. 5 with K replaced by ΔK, σ_y by $2\sigma_y$, and δ replaced by $\Delta\delta$.

It is deduced from Figs. 12*a* and *b* that for $R = 0$ and 0.5 a growing fatigue crack in either geometry displays a cyclic crack opening response $\Delta\delta$ closer to that of a stationary crack than that of a tearing crack. For the bend specimen at $R = 0$, $\Delta\delta$ is unchanged as Δa is increased from $0.080\ K_{max}^2/\sigma_y^2$ to $0.414\ K_{max}^2/\sigma_y^2$. For the CCP geometry at $R = 0$, $\Delta\delta$ increases with increasing Δa as the crack tip grows away from the residual hump of material on the crack flanks near a_o. Now consider the case of $R = 0.8$. The fatigue crack in both geometries unloads and reloads like an elastic crack since only a few elements experience reversed yield at the crack tip. A much finer mesh is required to elucidate the $\Delta\delta$ response when K_{min} is close to K_{max}.

It is clear from the above results and discussion that a growing fatigue crack is quite different from a stationary crack in the manner it opens and shuts. Its crack opening response is a function of load ratio, geometry, and crack growth increment.

Definition of the crack tip opening displacement δ^{tip} is difficult for the case of a growing fatigue crack at high R, since $\delta \to 0$ as the distance from the crack tip, $x \to 0$. Rice [12] has suggested that the crack tip opening displacement is defined by the intersection of the crack opening profile δ versus x, and the line $\delta/2 = |x|$. Unfortunately this procedure cannot be used for the growing fatigue crack (or the tearing crack) as the δ_{max} versus x curve is not sufficiently steep near the crack tip to give an intersection point. Therefore, δ^{tip} is defined arbitrarily as the value of δ at $x = -0.01\ K_{max}^2/\sigma_y^2$. The maximum crack tip opening displacement $\delta_{max}{}^{tip}$ at K_{max} and the minimum crack tip opening displacement $\delta_{min}{}^{tip}$ at K_{min} are given in Fig. 13 as a function of load ratio R and geometry. Values for $R = -1$ and $R = 0.3$ are included, though not discussed elsewhere in this paper. It is deduced that crack closure does not occur in the CCP specimen at $R = 0.3$ as the crack is closed over only a single element dimension at minimum load of the fatigue cycle. The crack opening load transient at $R = -1$ is approximately the same as at $R = 0$ for both geometries.

It is clear from Fig. 13 that $\delta_{max}{}^{tip}$ is not constant with respect to R but decreases with increasing R for both geometries. For $R > 0$, $\delta_{max}{}^{tip}$ and $\delta_{min}{}^{tip}$ are greater for the bend specimen than for the CCP geometry, while the cyclic crack tip opening displacement $\Delta\delta^{tip}$ $(= \delta_{max}{}^{tip} - \delta_{min}{}^{tip})$ is the same for both types of specimen. At $R = -1$, $\delta_{max}{}^{tip}$ and $\Delta\delta^{tip}$ are slightly greater for the CCP specimen than for the bend specimen. As R tends to 1 the fatigue crack becomes a tearing crack, and $\delta_{max}{}^{tip}$ and $\delta_{min}{}^{tip}$ tend to the tearing crack solution.

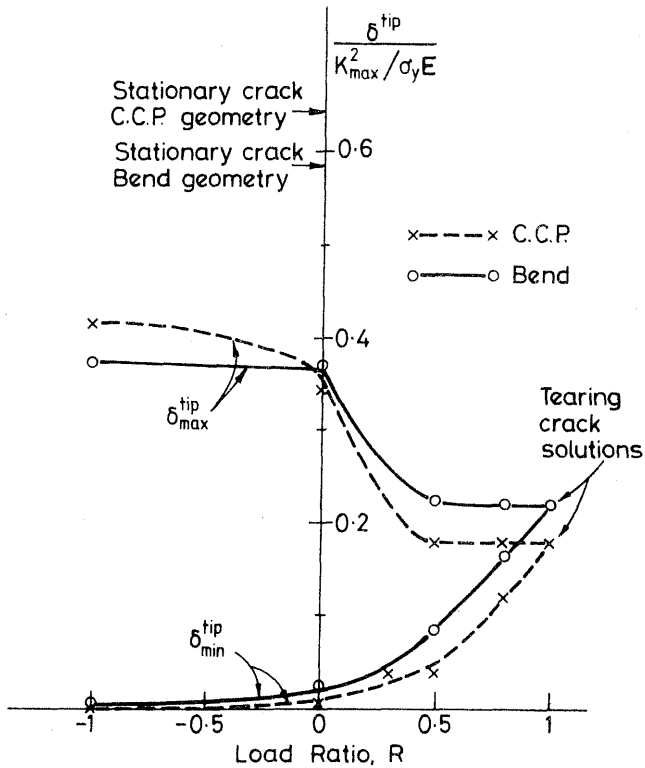

FIG. 13—*Crack tip opening displacement* δ^{tip} *for a growing fatigue crack.* δ^{tip} *is defined arbitrarily as* δ *at a distance of 0.01* K_{max}^2/σ_y^2 *behind the crack tip.* $\Delta a = 0.080\ K_{max}^2/\sigma_y^2$.

Plastic Zone Distribution for Growing Fatigue Crack

The plastic zones at K_{max} and K_{min} are plotted for each load ratio in Figs. 14*a* through *d* for the CCP geometry and in Figs. 15*a* through *d* for the bend specimen. Results are given for a crack growth increment Δa of $0.080\ K_{max}^2/\sigma_y^2$ and also for $\Delta a = 0.414\ K_{max}^2/\sigma_y^2$ for the case of $R = 0$.

For all cases considered in Figs. 14 and 15, the plastic zone ahead of the crack tip at K_{max} is similar in size to that of the corresponding tearing crack (Figs. 6*a* and *b*) under the same K_{max}. Also, the reversed plastic zone ahead of the crack tip at K_{min} is similar to that of the stationary crack at K_{min}. Here, comparisons are made for the same geometry and for the same R value.

Now consider the secondary active plastic zone along the crack flanks of the bend specimen (Figs. 15*a* through *d*). For $R = 0.8$ and 0.5 at $K = K_{max}$, this zone is similar to that of the tearing crack given in Fig. 6*b*; within this zone $\sigma_{xx} \approx \sigma_y$, $\sigma_{xx} \approx 0 \approx \tau_{xy}$. At $R = 0$ this secondary plastic zone is much diminished in size and extends from just behind a_o to about $0.06\ K_{max}^2/\sigma_y^2$ from the crack tip, (Figs. 15*c* and *d*). For all R and Δa, the secondary plastic zone along the crack flanks disappears at K_{min}. These results are consistent with the observation that T/σ_{nom} is positive for the bend geometry. At K_{max}, the T-stress reinforces the secondary plastic zone size; on unloading to K_{min}, the corresponding change in T-stress causes material along the crack flanks to unload elastically from the yield surface.

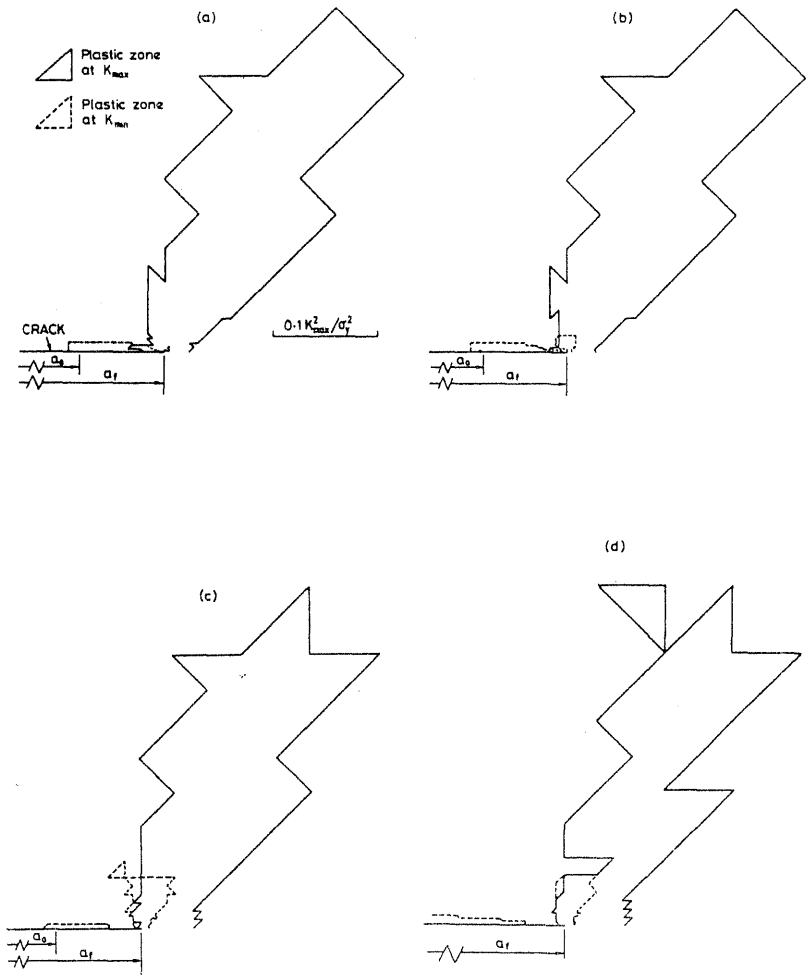

FIG. 14—*Active plastic zones at* K_{max} *and at* K_{min} *for growing fatigue crack in CCP geometry:* (a) R = *0.8*, $\Delta a = 0.080\ K_{max}^2/\sigma_y^2$, (b) R = *0.5*, $\Delta a = 0.080\ K_{max}^2/\sigma_y^2$; (c) R = *0*, $\Delta a = 0.080\ K_{max}^2/\sigma_y^2$, *and* (d) R = *0*, $\Delta a = 0.414\ K_{max}^2/\sigma_y^2$.

Now consider the CCP specimen (Figs. 14*a* through *d*). Here, the secondary plastic zone appears at K_{min}, not K_{max}. This is consistent with the fact that T/σ_{nom} is negative for this geometry. On unloading from K_{max} to K_{min} the change in T/σ_y is positive, leading to an active yield zone along the crack flanks at K_{min}, with $\sigma_{xx} \approx \sigma_y$, $\sigma_{yy} \approx 0 \approx \tau_{xy}$. On reloading to K_{max} the change in T/σ_y is negative, and material along the crack flanks unloads elastically.

Examination of Figs. 14*a* through *d* and 15*a* through *d* shows that the size of the secondary plastic zone at K_{min} decreases with decreasing R; for $R = 0$, it is a thin region extending from just behind a_o to $0.04 \pm 0.02\ K_{max}^2/\sigma_y^2$ from the crack tip. It is thought that reversed plasticity at the crack tip decreases the magnitude of the residual plastic strains in the wake of the advancing crack tip, and thereby decreases the size of the secondary plastic zone along the crack flanks. Hence the size of the secondary plastic zone decreases with decreasing R. This argument is supported by the observation that the state in a substantial fraction of

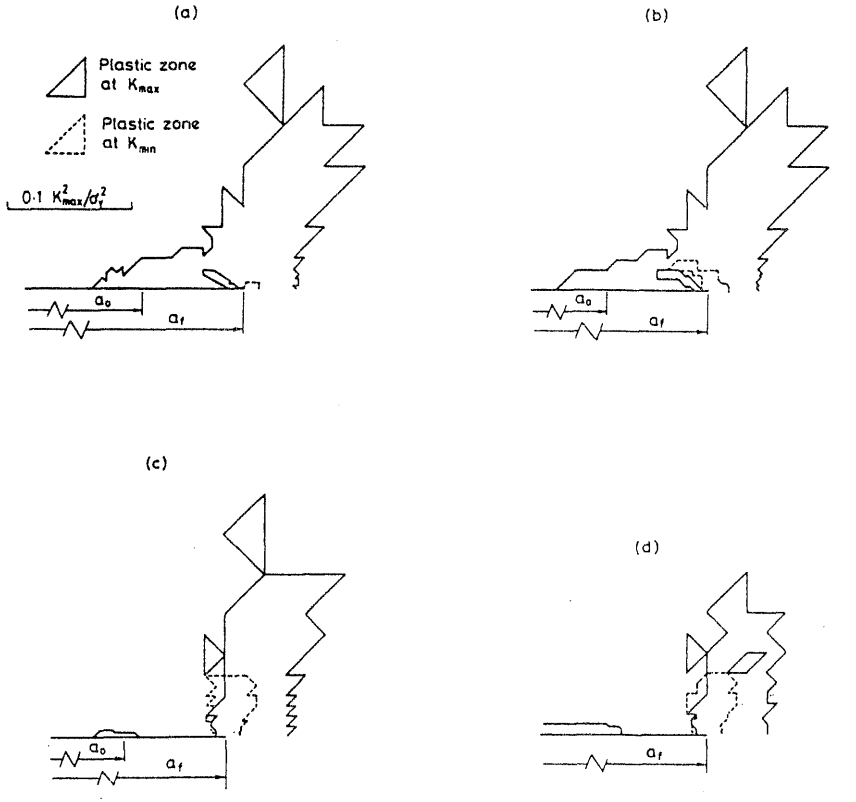

FIG. 15—*Active plastic zones at* K_{max} *and at* K_{min} *for growing fatigue crack in bend geometry:* (a) R = *0.8,* $\Delta a = 0.080\ K_{max}^2/\sigma_y^2$, (b) R = *0.5,* $\Delta a = 0.080\ K_{max}^2/\sigma_y^2$; (c) R = *0,* $\Delta a = 0.080\ K_{max}^2/\sigma_y^2$, *and* (d) R = *0,* $\Delta a = 0.414\ K_{max}^2/\sigma_y^2$.

the reversed plastic zone at the tip of the growing fatigue crack is approximated by $\sigma_{xx} = \sigma_{yy} + \sigma_y$, $\tau_{xy} = 0$, and the cyclic plastic strain in the thickness direction $\Delta\epsilon_{zz}^{pl} = 0$. This state corresponds to tensile yield in the x-direction and exists along a ray from the crack tip at an angle θ of approximately 80° (Figs. 16*b* and *d*). Similarly, tensile yield in the x-direction occurs within the reversed plastic zone for a stationary crack; material elements that suffer this stress state are also located along a ray from the crack tip, but at an angle θ of approximately 60° (Figs. 16*a* and *c*). Asymptotic analyses of the stress state at a crack tip for a stationary crack suggest that tensile yield in the x-direction occurs in a sector emanating from the crack tip with boundaries $\theta = 0°$ and $\theta = 45°$. Clearly, more work is required to elucidate the form of the stress-strain fields near the tip of stationary and growing cracks under cyclic loading.

Concluding Discussion

Several novel features have been observed about the nature of stationary and growing plane strain cracks under static and cyclic loading. Specimen geometry has an influence on the crack opening response and on the plastic zone distribution of a stationary crack, a tearing crack, and a growing fatigue crack. Larsson and Carlsson [*3*] have shown that the influence

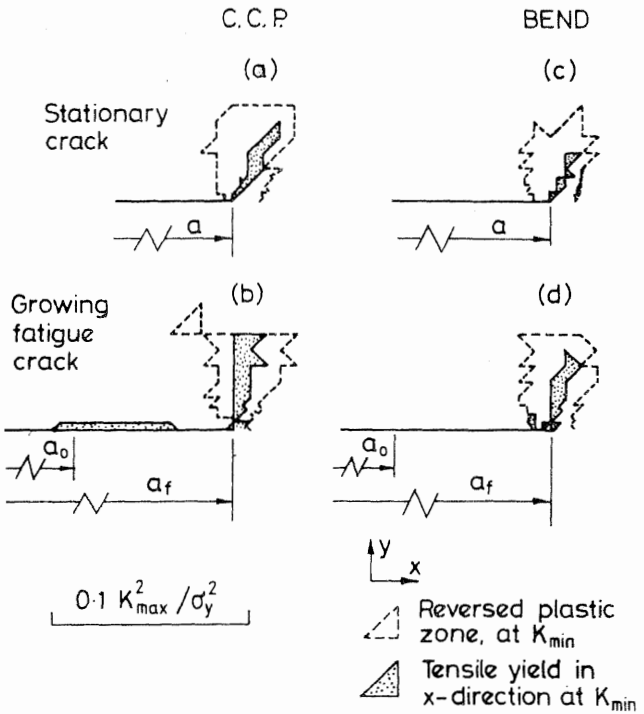

FIG. 16—*Examination of the active plastic zone at* K_{min} *for a stationary crack during first load cycle and for a growing fatigue crack after 20 crack growth increments* ($\Delta a = 0.080\ K_{max}^2/\sigma_y^2$). $K_{max} = 0.44\ \sigma_y \sqrt{w}$, $K_{min} = 0$.

of specimen geometry upon the response of a statically loaded stationary crack can be accounted for in terms of the T-stress parallel to the crack flanks, from the elastic solution. It is postulated that this T-stress can also account for the variation in behavior of tearing cracks and growing fatigue cracks with specimen geometry.

Plasticity-induced crack closure only occurs in plane strain under transient conditions, as a crack evolves from a stationary state to the steady state of a growing fatigue crack. For the CCP geometry, a residual wedge of stretched material is left on the crack flanks at the location of the maximum plastic zone associated with the initial crack. This residual wedge of material leads to a maximum value of P_{op}/P_{max} of about 0.3, when the crack has advanced by about 0.15 K_{max}^2/σ_y^2. With further crack advance P_{op}/P_{max} falls steadily to zero, and the crack displays discontinuous closure. Such plasticity-induced closure does not occur in the CCP geometry at higher R, or in the bend specimen at $R \geqq 0$. These observations relate to computations where K_{max} is held constant at $0.44\ \sigma_y \sqrt{w}$, which is just below the ASTM limit for small-scale yielding (ASTM E 399). At lower values of K_{max} the ratio T_{max}/σ_y is less different for the bend and CCP geometries, where T_{max} is the T-stress from the elastic solution corresponding to K_{max}. It is argued that the ratio T_{max}/σ_y accounts for the influence of specimen geometry upon the solution for a growing fatigue crack. Hence, it is predicted that differences between the closure response of the CCP and bend geometries are decreased with decreasing K_{max}. This is confirmed elsewhere [*13*].

An examination of the crack opening behavior and the plastic zone distribution at the tip of a growing fatigue crack suggests that this type of crack is different from a stationary crack

and from a tearing crack. In approximate terms, the growing fatigue crack at K_{max} bears some similarity to a tearing crack, while the cyclic response of a growing fatigue crack bears more resemblance to that of a stationary crack. Since the nature of the crack tip singularity for the growing fatigue crack appears to be different from that of a stationary crack, crack tip singularity elements corresponding to the stationary crack solution should not be used in a finite-element analysis of fatigue crack growth. The triangular elements used in the present study have the ability to accommodate, albeit approximately, the actual singularity existing at the tip of an advancing fatigue crack.

In the present study it is found that the cyclic crack opening response $\Delta\delta$ of a growing fatigue crack is independent of specimen geometry provided crack closure does not occur. If it is assumed that the fatigue crack growth rate da/dN is a unique function of $\Delta\delta$ at the crack tip, then it is deduced that specimen geometry had little effect upon fatigue crack growth rate, unless tests are performed at a sufficiently low load ratio for crack closure to be significant. The experimental observations of Kitigawa et al. [*14*] support this conclusion.

Acknowledgments

One of the authors (NAF) is grateful to the U.S. National Research Council for funding in the form of a Research Associateship. Both authors wish to thank the Director of NASA Langley Research Center for the provision of computing facilities.

References

[*1*] Tada, H., Paris, P. C., and Irwin, G. R., *The Stress Analysis of Cracks Handbook,* Del Research Corporation, 1973.

[*2*] Dean, R. H. and Hutchinson, J. W., in *Fracture Mechanics: Twelfth Conference, STP 700,* American Society for Testing and Materials, Philadelphia, 1980, pp. 383–405.

[*3*] Larsson, S. G. and Carlsson, A. J., J. Mech. Phys. Solids. Vol. 21, 1973, 263–277.

[*4*] Rice, J. R., *Journal of Mechanics and Physics of Solids,* Vol. 22, 1974, pp. 17–26.

[*5*] Nagtegaal, J. C., Parks, D. M., and Rice, J. R., *Computer Methods in Applied Mechanics and Engineering,* Vol. 4, 1974, pp. 153–177.

[*6*] Newman, J. C., Jr, *Mechanics of Crack Growth, STP 590,* American Society for Testing and Materials, Philadelphia, 1976, pp. 281–301.

[*7*] Sham, T.-L., in *Elastic Plastic-Fracture: Second Symposium, Volume I: Inelastic Crack Analysis, STP 803,* C. F. Shih and J. P. Gudas, Eds., American Society for Testing and Materials, Philadelphia, 1983, pp. I.52–I.79.

[*8*] Rice, J. R., *Fatigue Crack Propagation, STP 415,* American Society for Testing and Materials, Philadelphia, 1967, pp. 247–311.

[*9*] Rice, J. R. in *Fracture—An Advanced Treatise, Mathematical Fundamentals,* Vol. II, H. Liebowitz, Ed., Academic Press, New York, 1968, pp. 191–311.

[*10*] Drugan, W. J., Rice, J. R., and Sham, T.-L., *Journal of Mechanics and Physics of Solids,* Vol. 31, No. 6, 1982, pp. 447–473; correction in *Journal of Mechanics and Physics of Solids,* Vol. 32, No. 2, 1983, p. 191.

[*11*] Ogura, K., Ohji, K., and Honda, K., in *Fracture 1977, Vol. 2, ICF4,* Waterloo, Canada, 19–24 June 1977, pp. 1035–1047.

[*12*] Tracey, D. M., *Journal of Engineering Materials and Technology, Transactions of the ASME,* Vol. 98, April 1976, pp. 146–151.

[*13*] Fleck, N. A., *Engineering Fracture Mechanics,* Vol. 25, No. 4, 1986, pp. 441–449.

[*14*] Kitigawa, H., Yuuki, R., and Tohgo, K., *Fatigue of Engineering Materials and Structures,* Vol. 2, 1979, pp. 195–206.